THE AMERICAN SOCIETY OF MECHANICAL ENGINEERS
345 E. 47th St., New York, N.Y. 10017

94-GT-387

PRE-STALL BEHAVIOR OF SEVERAL HIGH-SPEED COMPRESSORS

M. Tryfonidis, O. Etchevers, J. D. Paduano, and A. H. Epstein
Gas Turbine Laboratory
Massachusetts Institute of Technology
Cambridge, Massachusetts

G. J. Hendricks
United Technologies Research Center
East Hartford, Connecticut

ABSTRACT

High speed compressor data immediately prior to rotating stall inception are analyzed and compared to stability theory. New techniques for the detection of small amplitude rotating waves in the presence of noise are detailed and experimental and signal processing pitfalls discussed. In all nine compressors examined, rotating stall precedes surge. Prior to rotating stall inception, all the machines support small-amplitude (<1% of fully developed stall) waves travelling about the circumference. Travelling wave strength and structure are shown to be a strong function of corrected speed. At low speeds, a ~0.5 times shaft speed wave is present for hundreds of rotor revolutions prior to stall initiation. At 100% speed, a shaft speed rotating wave dominates, growing as stall initiation is approached (fully developed rotating stall occurs at about 1/2 of shaft speed). A new, 2-D, compressible hydrodynamic stability analysis is applied to the geometry of two of the compressors and gives results in agreement with data. The calculations show that, at low corrected speeds, these compressors behave predominantly as incompressible machines. The wave which first goes unstable is the 1/2 shaft frequency mode predicted by the incompressible Moore-Greitzer analysis and previously observed in low speed compressors. Compressibility becomes important at high corrected speeds and adds axial structure to the rotating waves. At 100% corrected speed, it is one of these hitherto unrecognized compressible modes which goes unstable first. The rotating frequency of this mode is constant and predicted to be approximately coincident with shaft speed at design. Thus, it is susceptible to excitation by geometric nonuniformities in the compressor. This new understanding of compressor dynamics is used to introduce the concept of travelling wave energy as a measure of compressor stability. Such a wave energy-based scheme is shown to consistently give an indication of low stability for significant periods (100-200 rotor revolutions) before stall initiation, even at 100% corrected speed.

INTRODUCTION

A recent focus of rotating stall research has been the inception process. Using both models and experimental data, researchers have attempted to develop an improved description of rotating stall inception, including the connection between small and large-amplitude disturbances, and between stall and surge. Such a description would be useful in several arenas, including compressor design, stall warning and avoidance, and stall control (both active and passive).

In past practice, experimental studies of stall inception used few sensors per stage, and concentrated on understanding local blade-row phenomena during stall inception. A more recent method for studying rotating stall inception, motivated by a hydrodynamic theory of compressor stability developed by Moore and Greitzer (1986), was first introduced by McDougall (1989). This method uses a circumferential array of sensors at one or more axial locations, and attempts to detect circumferential waves of perturbation pressure or velocity. Hydrodynamic theory predicts that sinusoidal rotating waves will become underdamped near the stall inception point, and thus spatial sinusoids should be detectable at small amplitudes before

Presented at the International Gas Turbine and Aeroengine Congress and Exposition
The Hague, Netherlands — June 13–16, 1994
This paper has been accepted for publication in the Transactions of the ASME
Discussion of it will be accepted at ASME Headquarters until September 30, 1994

stall inception occurs. This information about the *spatial structure* of the pre-stall disturbances provides a guideline for combining multiple measurements. The subsequent improvement in signal-to-noise ratio potentially allows detection of low amplitude pre-stall waves which would otherwise be missed in the noisy compressor environment.

Two questions have been raised concerning this approach to stall warning. First, it is important to understand whether, and under what conditions, spatial waves exist in high-speed axial compressors prior to stall inception. Clearly one cannot take advantage of the predicted temporal and spatial structure if this structure does not exist. Second, if waves exist, what are the best methods to detect them and to transform detection into an incipient stall warning signal?

The question of wave existence has been studied by several researchers, including Garnier (1991), Day, (1993a, 1993c), Gallops (1993) Hoying (1993), Boyer et al. (1993), and Freeman and Wilson (1993). In this paper, we will present data from several compressors, some of which were studied previously by other investigators. Our approach is to show characteristics that are similar across a variety of high speed compressors using common analysis tools and to connect these experimental observations with hydrodynamic stability theory.

It is important at the outset to distinguish the terminology that we will use. *Fully developed rotating stall* refers to the large amplitude (50~100% mass flow fluctuations) rotating stall, during which amplitude variations of the perturbations are insignificant. *Stall inception* is the transient from axisymmetric, small perturbation flow conditions to rotating stall, and thus includes large disturbances whose amplitudes change with time. The short wavelength disturbances reported by Day (1993a) fall into this category. *Pre-stall* refers to the period of time immediately prior to stall inception, during which compressor operation is steady but may exhibit small amplitude (on the order of 1%) dynamics. Perturbations associated with these dynamics are small compared both to stall inception and to fully developed stall perturbations. These three regions — pre-stall, stall inception, and fully developed stall — are difficult to separate precisely; rather the terminology allows us to communicate the ideas presented in the paper in a more concise manner. (Examples of delineating data in this way are given in Fig. 3, to be discussed in a later section.)

The stable, pre-stall inception region is in many ways the most interesting since stable operation is the design goal, a goal that is lost once stall initiates. Yet compressor dynamics in this region has been little studied. Therefore, our focus is on the pre-stall inception dynamics of high speed compressors, attacked with theory and experiment.

In the following sections, we will present a new data reduction procedure which reveals the presence of small amplitude, pre-stall travelling waves in all of the compressor studied. This wave structure is shown to be a strong function of corrected speed. The results of a new, compressible, hydrodynamic stability model are given which are in agreement with the data. The calculations indicate that the speed dependence of the wave structure is due to the effects of compressibility at the higher rotational speeds. This understanding of high speed compressor wave structure adds a new perspective to real-time stall warning prospects. Promising results of a wave energy-based scheme are presented. We close by discussing the implications of compressible wave structure and dynamics for compressor design.

DATA REDUCTION PROCEDURES

Since one of our primary goals in this paper is to investigate the existence of pre-stall waves in high speed compressors, our data reduction procedures are purposefully designed to avoid pre-disposition of the results. Thus, for instance, we do not narrow-band pass filter the data, as this can yield spurious travelling when very little actual wave energy exists. In fact, we do not in any way take advantage of the predicted (and, often, measured) *temporal* structure of the waves in our initial analysis; presumably doing so (for instance, by doing model-based filtering such as Kalman filtering) would improve at least the appearance of the results.

We do take advantage, in some of our data reduction, of the *spatial* structure of the predicted travelling waves, and this provides a way to detect travelling of spatially coherent structures. Following the theoretical development of Garnier (1991), we assume that the pressure perturbations of interest take the following form at a given axial station:

$$\delta P_x(\theta,t) = \mathrm{Re}\left\{ \sum_{k=-\infty}^{\infty} a_k(t) \cdot e^{ik\theta} \right\} \qquad (1)$$

where x indicates the axial station at which the measurements are taken, and $a_k(t)$ are the *spatial* Fourier coefficients of the perturbations. According to linearized hydrodynamic theory of compressor stability, the spatial Fourier coefficients evolve independently and thus constitute the fundamental states of the system. (In contrast, the pressure perturbation $\delta P_x(\theta_n, t)$ at a given circumferential position θ_n is correlated to that at any other position, and thus constitutes an amalgam of dynamic effects which must somehow be distinguished.)

We can derive an approximation for $a_k(t)$ from a set

of N circumferential measurements of δP_x by using the spatial Fourier transform:

$$a_k(t) = \frac{1}{N}\sum_{n=1}^{N} \delta P(\theta_n, t)\cdot \exp(-2\pi i k\theta_n) \qquad (2)$$

where N must obey the Nyquist criterion for the mode k, that is, $N \geq 2k+1$. The sensor locations θ_n are often, but not necessarily, evenly spaced; even or nearly-even spacing insures that harmonics *below* the Nyquist do not alias into the estimate of $a_k(t)$.

If our assumption about the independence of spatial harmonics is correct, then we have effectively diagonalized the system, and the states $a_k(t)$ can be treated as evolving according to independent dynamics. This data reduction procedure assumes very little about what these dynamics are, but since we are searching for such dynamics it is important at this point to describe the expected behavior. In the low-speed (Garnier, 1991) hydrodynamic model, a single eigenvalue usually dominates at a given operating point and thus a simple model of spatial Fourier coefficient evolution is expected (see, for instance, Garnier):

$$\frac{da_k}{dt} = (\sigma_k - i\omega_k)a_k + V(t) \qquad (3)$$

where $V(t)$ represents random excitation of the system related to the unsteady aerodynamics of the compressor, inflow distortions, etc. Since the character of this noise is currently unknown in compressors and engines, we assume here white noise excitation. Figures 1 and 2 show the behavior of such a system, based on simulation of Eq. (3), in two different ways.

Figure 1 shows the time history of the magnitude and phase of the first spatial harmonic, $a_1(t)$ for various values of the damping ratio, $\zeta = \sigma_k / |\sigma_k + i\omega_k|$, which goes to zero as the compressor approaches the instability point. The magnitude is the wave strength, while the phase is the wave angular position in the compressor annulus. The linear dynamics of the modeled compressor exhibit a gradual trend towards coherent travelling as the damping ratio decreases. However, the damping ratio is quite small here before travelling is absolutely deterministic in appearance (i.e., before the phase history is a straight line, Fig. 1c), and the magnitude of the waves at this point is correspondingly large. These results assume that there is no corrupting measurement noise in the data, so we expect that the damping ratio must indeed be quite small in order for a coherent, deterministic wave to be detected in the presence of both process and measurement noise.

Figure 2 shows the spatial power spectra (PSD of a_1) averaged over a period corresponding to each of the damping ratios in Fig. 1. Note that $a_k(t)$ is a complex function of time, so the power spectrum is *not symmetric about zero spatial frequency*, $\omega = 0$. This lack of symmetry allows us

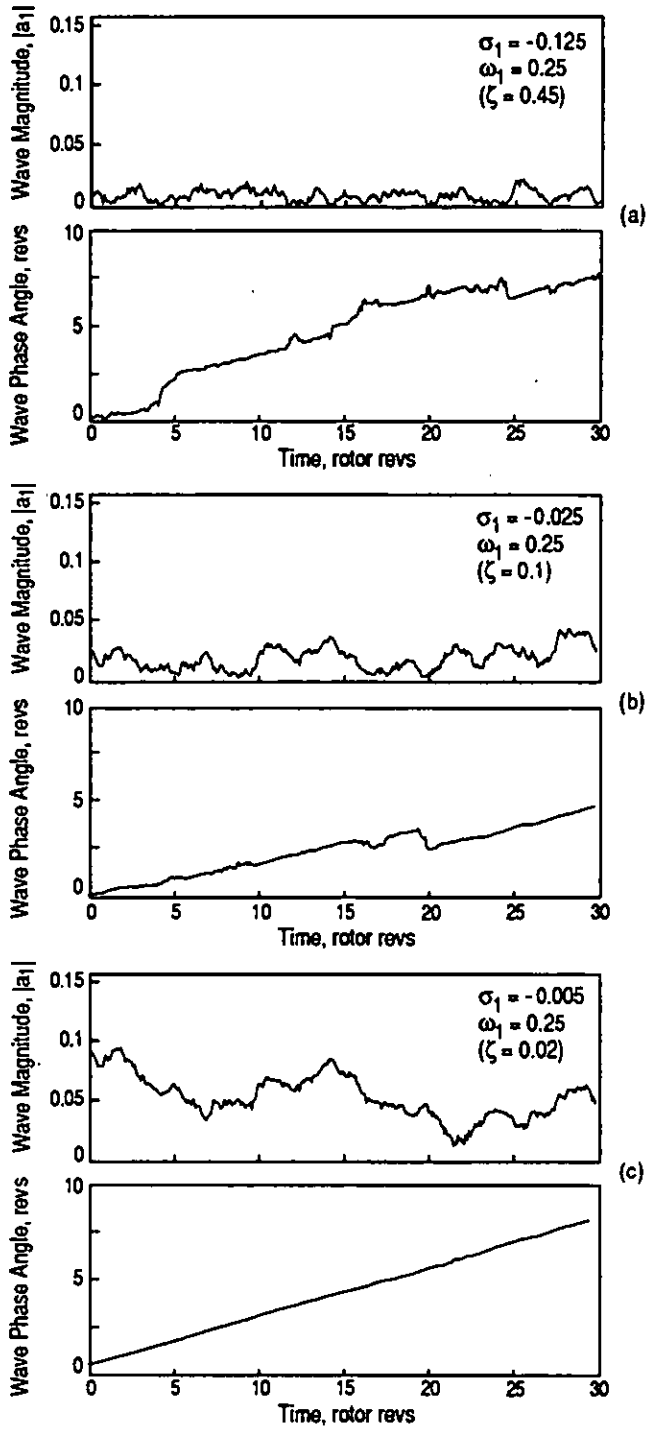

Fig. 1: Simulated compressor 1st Fourier harmonic wave amplitude and phase behavior, based on Eq. (3).

to distinguish between standing waves oscillating in amplitude, and rotating waves with constant amplitude (see Appendix A); standing waves yield no difference between positive and negative frequencies, while travelling waves show asymmetric peaks, which we term 'travelling wave energy' in the spectrum. This distinction can be quite useful. The integral difference between the positive and negative spectra (the shaded area in Fig. 2) is a quantitative measure of the travelling wave energy which exists in the compressor over a given interval of time. In a noisy environment, an *integral* measure of travelling wave energy can be a more sensitive detector of wave existence than *differential* schemes such as depending on straight line behavior of spatial phase plots. This is clearly illustrated by this simulation. At the higher damping ratios (ξ = 0.45 to 0.1), the evidence for travelling waves is ambiguous in the phase plots in Fig. 1, but travelling energy is readily apparent in the spatial power spectra of Fig. 2 at the same conditions (for more details see Etchevers, 1992).

The procedures outlined above can be compromised to various degrees by the existence in most data of relatively large amounts of travelling wave energy at multiples of the rotor frequency. This energy is due both to geometric excitation and the response of the compressor dynamics to that excitation. It may be desirable at times to eliminate this rotor frequency energy since its large amplitude can obscure other frequencies. In this case, a narrow-band notch filter of some type must be implemented. We utilize a feed-forward adaptive LMS approach (Widrow, 1975) to do this for two reasons: first, it allows slow variations in the rotor frequency to be automatically tracked (important for real-time implementations), and second, it allows wave energy which is uncorrelated with the rotor passage to pass through (this effect could be implemented with a non-adaptive scheme, but not without some difficulty).

In this section, we have explained the motivation for several types of data reduction. Typically, one must examine the data from these various points of view to generate a complete picture of the behavior of the system. A typical set of data reduction steps is as follows:

1) Basic data preparation:
   a) Examine raw data for outliers and anomalies;
   b) Detrend the data to take out zero and very low frequency variations;
   c) Normalize root mean square fluctuations (across the circumferential array) to take out effects of miscalibration and sensor positioning.
2) Calculate spatial Fourier coefficients [for example, 8 probes => spatial Fourier coefficients 1, 2, and 3 using Eq. (2)]; plot phase and magnitude as functions of time.
3) When called for, eliminate oscillations which are highly correlated with rotor rotation rate (feed-forward adaptive LMS algorithm), or local to a few sensors.
4) Calculate power spectra of the *pre-stall* data; plot and compare positive and negative frequencies.
5) Compute integrated area difference between positive- and negative- frequency spectra.

Clearly, to plot all of the results from the above procedure for all of the compressors tested, for multiple trials, at their various operating condition, would fill a substantial volume. Here we will attempt to summarize the trends observed and characterize each compressor with respect to the current model of pre-stall compressor dynamics.

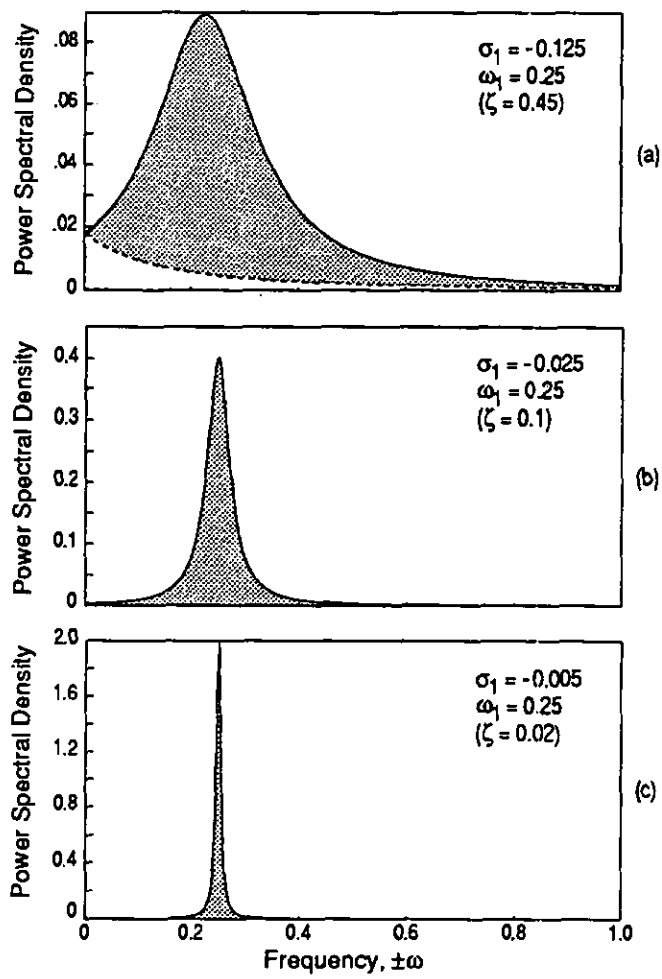

Fig. 2: Spatial spectra (PSD of a_1) of the simulations shown in Fig. 1. Solid line is the positive frequency spectrum, dotted line is the negative frequency (visible only in (a), close to zero in (b) and (c)). The shaded area difference between them is a measure of the travelling wave energy.

COMPRESSORS STUDIED

The high speed compressor data presented here were all taken by cooperating industrial and U.S. government organizations. The compressors studied cover over 30 years of design practice ranging from older and current engine designs to advanced concepts. Some are fixed geometry, some have interstage bleeds, and some have variable IGV's and stators. In the latter machines, the geometry of the compressor varies with operating speed. In all cases, data are time resolved wall static pressure measurements, roughly equally spaced around the annulus at one or more axial stations. In cases where more than one axial station was instrumented, the station which gave the best results is shown here. All data were taken in compressor test rigs except for #9. The following designations will be used:

Compressor No.	Description
#1	- 1-stage civil fan, nacelle in wind tunnel
#2	- 1-stage high throughflow military fan (Boyer, 1993)
#3	- 3-stage core compressor (Garnier, 1991)
#4	- 4-stage core compressor (Hoying, 1993)
#5	- 5-stage core compressor
#6	- 6-stage
#7	- 7-stage axial, 1-centrifugal, T-55 data (Owen, 1993)
#8	- 8-stage
#9	- 8-stage, Viper engine data (Day and Freeman, 1993c)

All compressors used 8 transducers about the circumference per station except #7 which had 4 transducers, and #9 which had 5. Geometry and steady-state performance data were provided for some of the compressors, facilitating comparison with theory; while for others, only normalized, unsteady, a.c. pressure traces were provided. For compressors with literature references, the data analyzed herein is not necessarily from that data set which appeared in previous publications.

STALL INCEPTION TRANSIENTS

The time-resolved transients into rotating stall are the rawest form of data we will present. Data for all 8 rig compressors are presented in Fig. 3, formatted primarily to indicate the similarities between the tests (for instance, the measurement units are varied arbitrarily to achieve similar magnitudes of the perturbations). Data are presented for the highest rotational speeds for which we have data, which in most cases is 100%. The main point to note is that distinct, large amplitude, rotating disturbances are seen in all of the compressors. We have generated over 100 such time histories for these and other compressors, at various operating conditions, and in all cases rotating perturbations exist prior to surge.

Note in Fig. 3 that most of the compressors tested (except #1 and #8) eventually exhibit planar, surge-type waves (which are sometimes followed by a transient due to opening of the downstream rig throttle, to prevent mechanical damage). Whether or not such surge instability occurs, however, all the compressors exhibit rotating disturbances first. Thus we conclude that rotating stall, and not surge, is the performance-limiting instability in axial compressors. Stated another way, if one were to stabilize or otherwise eliminate the surge mode of an engine, rotating stall would still occur, and no compressor range extension would be realized. This was demonstrated on a low-speed compression system by Greitzer et al. (1978).

Figure 3 also illustrates our delineation of pre-stall, stall inception, and fully developed stall (see the traces from Compressor 1 and Compressor 5). Most of the compressors tested begin to surge during stall inception. Thus coherent, fully-developed stall is never reached, and in these compressors we use the delineation pre-stall, stall/surge inception, and surge.

Another view of stall inception is provided by plotting time histories of the spatial Fourier coefficients, $a_k(t)$ of Eq. (2), during stall inception. This approach highlights circumferentially travelling phenomena, allowing smaller amplitude perturbations to be detected prior to stall. These data are presented in Fig. 4 for the same 100% speed tests as in Fig. 3 (rotor frequency has been filtered out here). The main point is that all the compressors show some evidence of rotating waves prior to stall – as straight line travelling on the phase plots and as increased amplitude on the magnitude plots. Figure 5 shows data taken at 70% speed for some of the compressors. At part speed, the travelling waves are evident for a longer time than at 100% speed.

The data in Figs. 4 and 5 clearly indicate that coherent rotating waves exist prior to stall. In addition to using this information to elucidate the fluid mechanics of stall inception in high speed compressors, it may be desirable to feed this "stall warning" information in real time to the engine fuel control for appropriate action to avoid stall (cutting back fuel, opening the nozzle or bleeds, repositioning the vanes, etc.). For stall avoidance based on rotating disturbance detection to be feasible, we must be capable of detecting disturbances sufficiently in advance of stall so as to permit the control system to take corrective action. Thus, there is motivation to optimize the analysis procedure so as to maximize the time over which waves can be detected.

Plots such as those in Figs. 4 and 5 can be used to

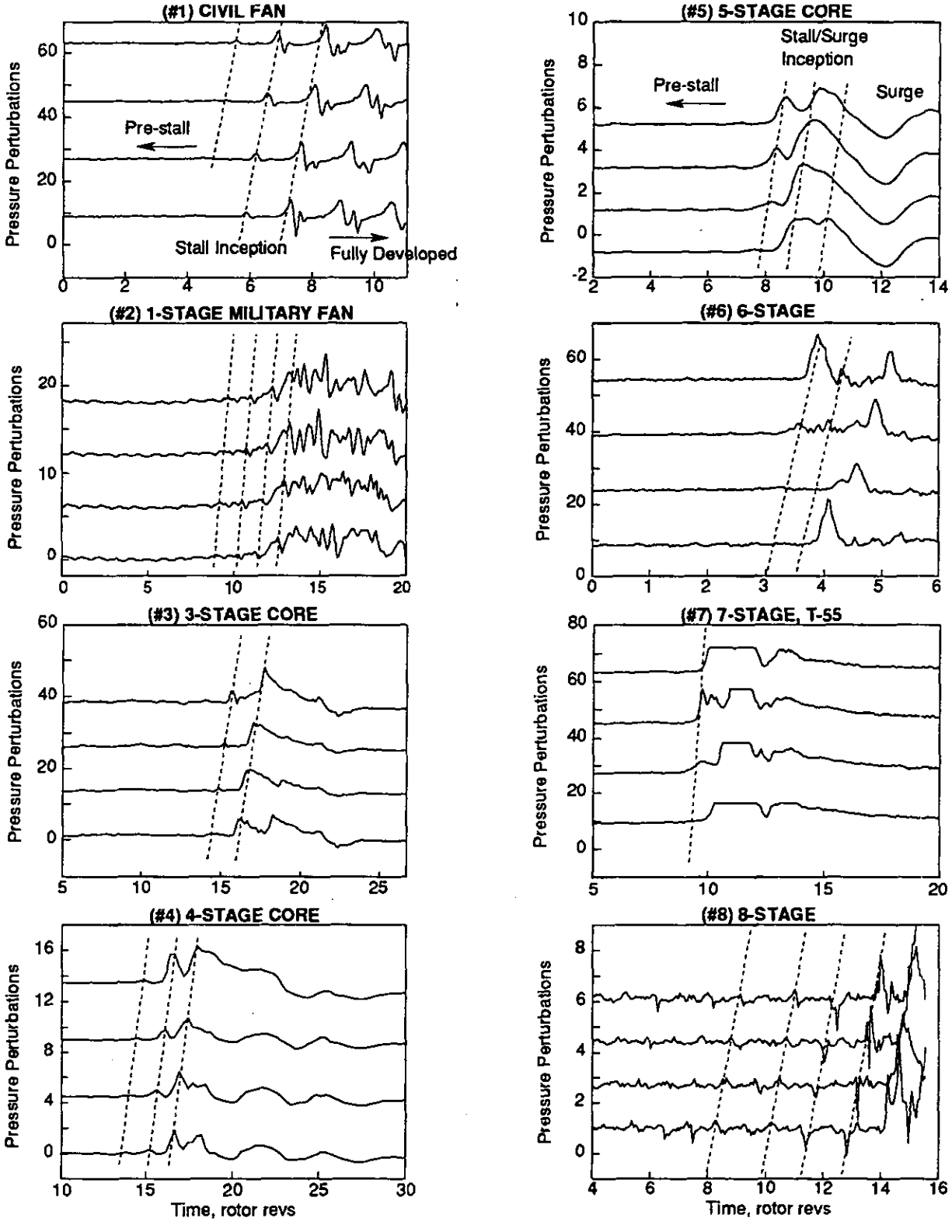

Fig. 3: Time traces of wall static pressure measured with 4 transducers equi-spaced about the compressor annulus during transients into stall/surge at 100% rotational speed. Data from 8 different compressors are shown. Compressors 1 and 5 are labeled with the terminology discussed in the text.

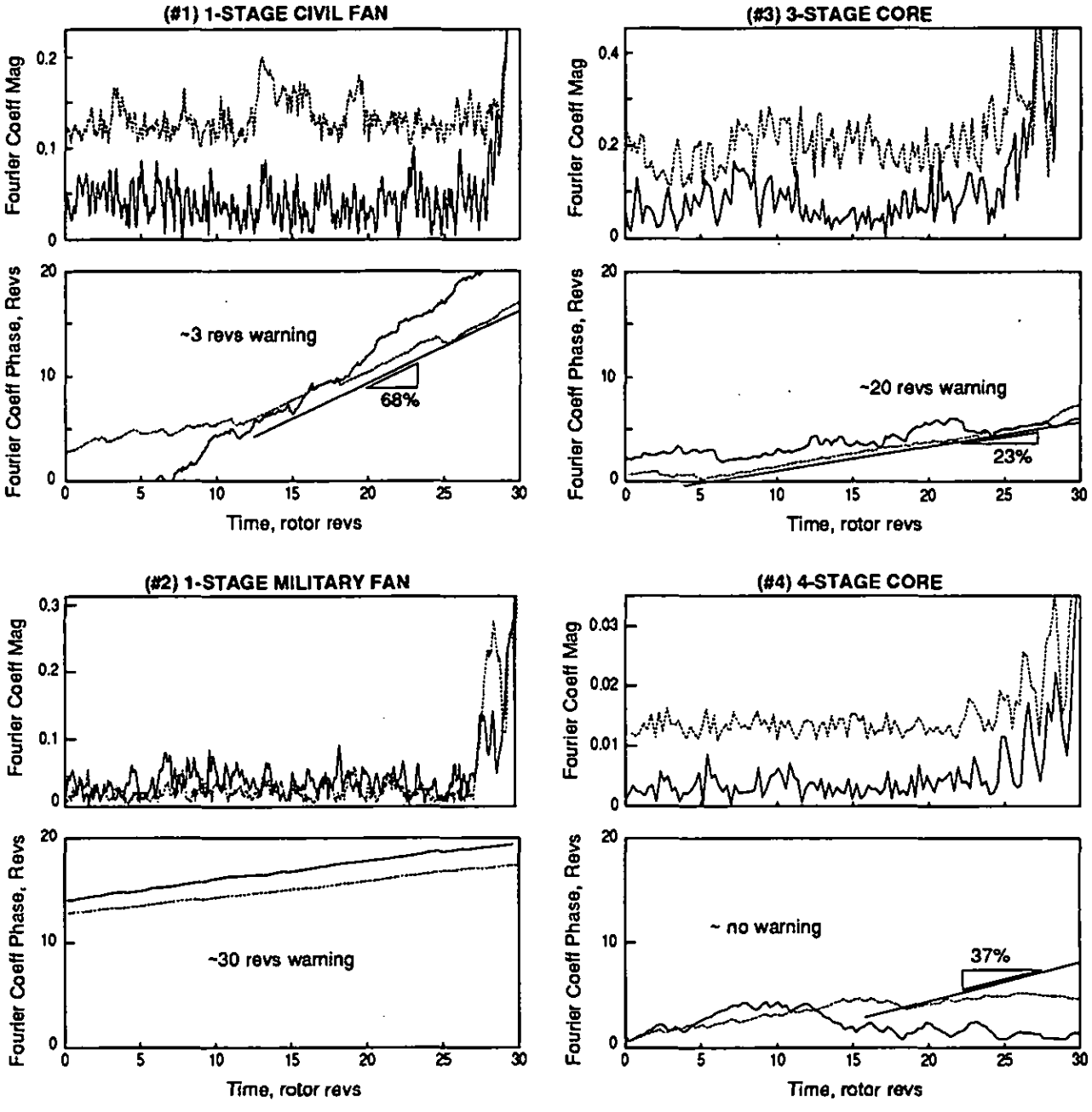

Fig. 4: First (solid line) and second (dotted line) spatial Fourier coefficients, a_1 and a_2, phase and magnitude immediately prior to stall/surge inception at 100% speed. The triangles indicate the speed at which the pre-stall wave travels about the compressor annulus (as a percent of rotor shaft speed).

determine a *very conservative* estimate of the period of time over which 'small amplitude' rotating waves exist prior to stall. One such procedure, described by Garnier (1991), is as follows: first, estimate the fully-developed rotating stall amplitude. Next, assume that waves are small if they are one eighth of this amplitude or smaller (this number is arbitrary but, again, conservative). Finally, determine the length of time for which the phase of the first or second Fourier harmonic exhibits straight-line (i.e. deterministic, coherent) motion prior to stall.

This is a very conservative approach for several reasons. In the simulation of Fig. 1, we showed that the wave

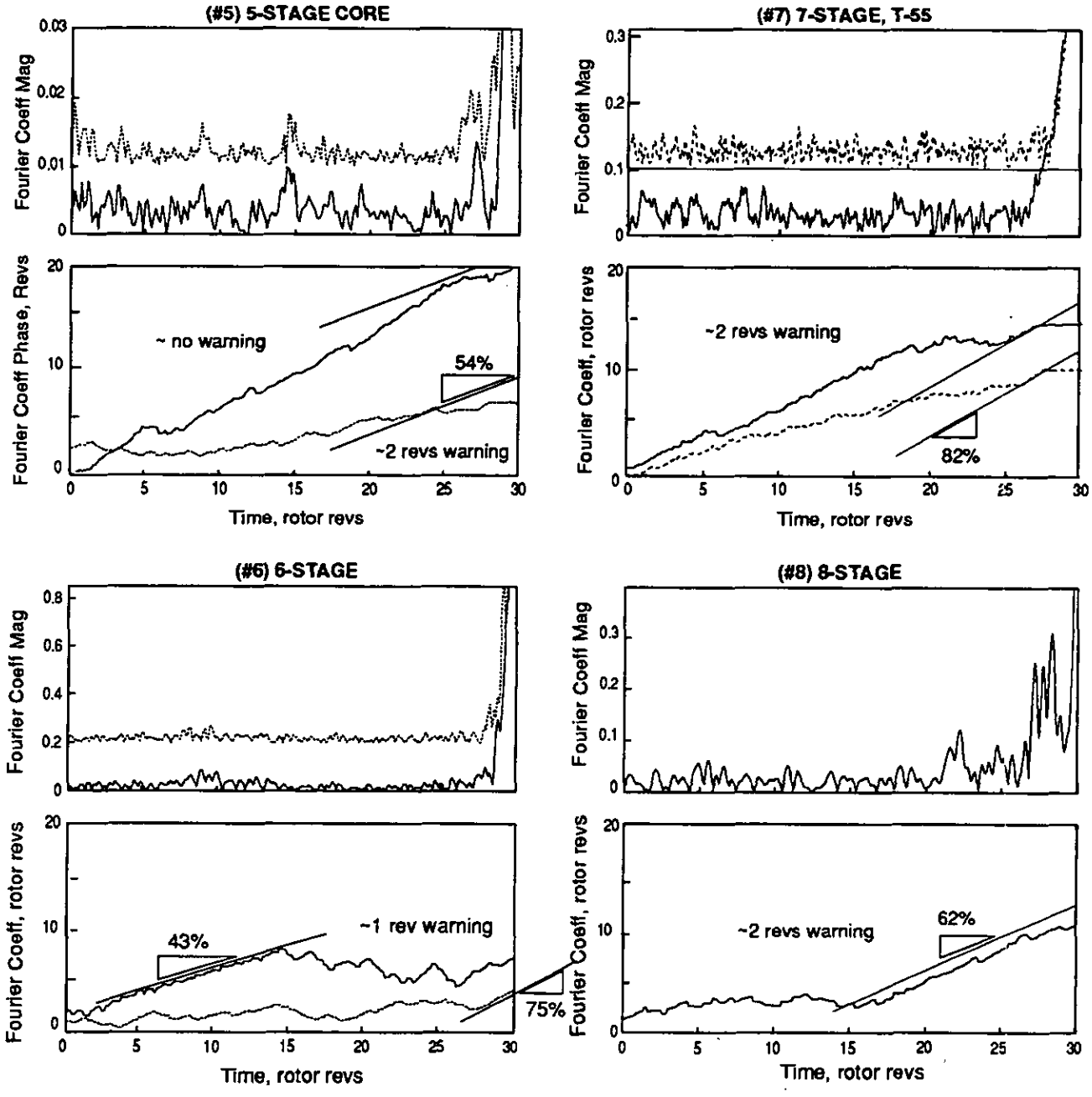

Fig. 4: Continued.

damping must be quite low for coherent travelling to be *apparent* even in the ideal simulation environment; at this point, however, the corresponding wave amplitudes may be sufficiently large to trigger stall. Exacerbating this problem is the noisy test environment, which can mask the desired wave structure. This is particularly troublesome for multi-stage compressor data taken with high-pressure, dc-coupled pressure transducers (as is the case for many of the compressors here), which may not have the sensitivity necessary to detect small amplitude waves when selected to survive surge in a high pressure compressor. (Some of this multi-stage data was taken with 50 or 100 psi full-scale pressure transducers; the pre-stall wave amplitudes detected here are only 0.05 psi.) It has also been shown (Mansoux et al., 1993) that nonlinear interaction between harmonics during stall inception often produces a period

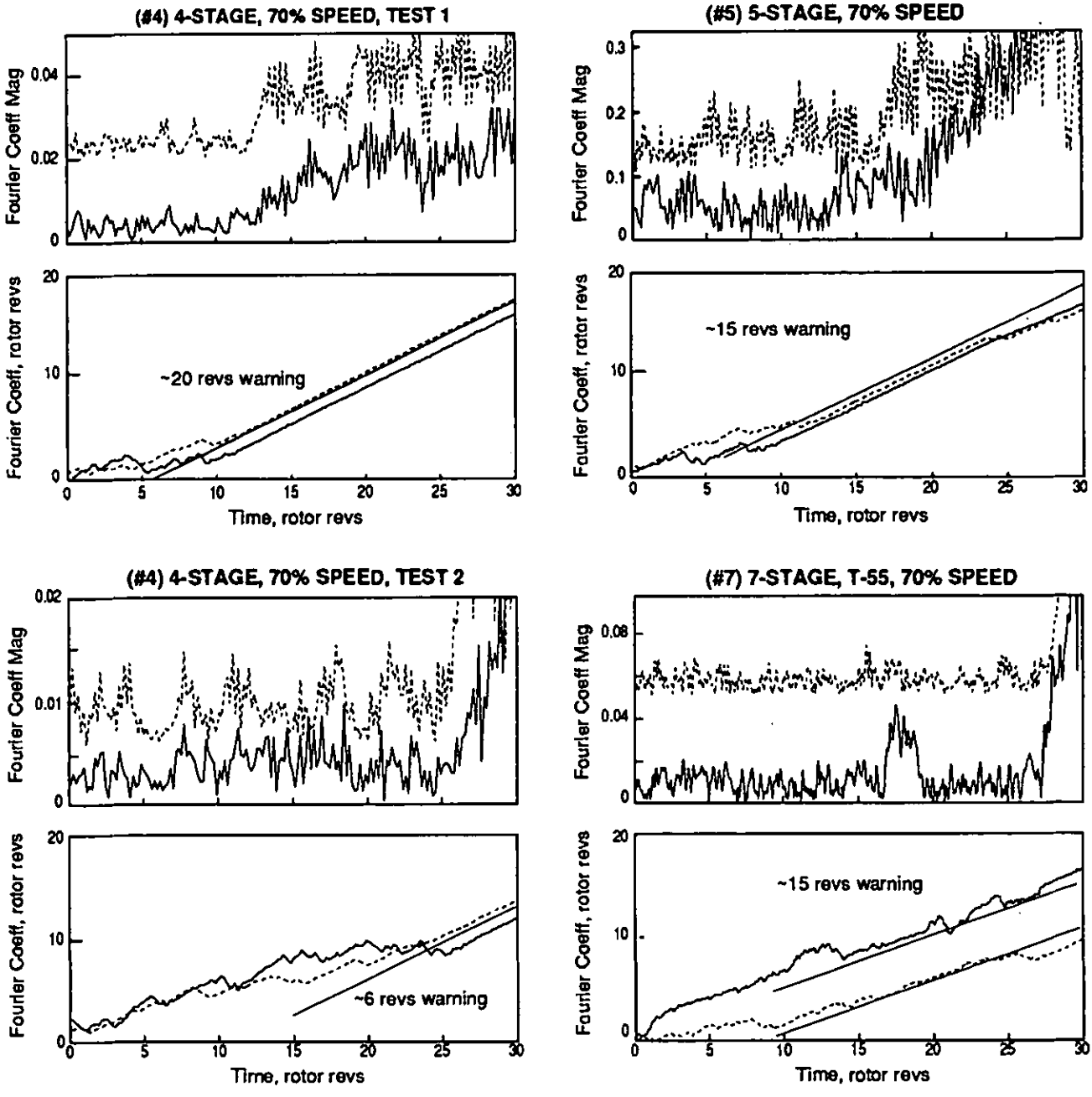

Fig. 5: Time history of first and second Fourier coefficients, as in Fig. 4 but at lower compressor rotational speeds.

during which wave energy is transferred between spatial harmonics. This behavior causes some wave amplitudes to shrink, while others grow. During the period that a given harmonic amplitude is small, its apparent phase can wander, both due to increased corruption by noise, and due to the nature of the nonlinear interaction. Thus, loss of apparent travelling during stall/surge inception is not evidence of the lack of existence of waves.

With these caveats in mind, 'stall warning' estimates are indicated on Figs. 4 and 5. We have chosen as the relevant measure the length of time over which *either* the first or the second harmonic travels in a straight-line fashion. For instance, in Fig. 4, compressors 1, 2, 3 and 7 exhibit distinct straight-line travelling of either the first or the second Fourier coefficient prior to stall. Thus in these cases it is unquestionable that pre-stall travelling waves exist. Stall

warning times, however, are 2 or 3 revs in some cases because of occasional periods of wandering phase. Compressors 4 and 5, on the other hand, show less distinct straight-line travelling, and this is reflected in the lack of any 'warning' time by this simple measure. Both of these plots show tendency to travel, but the results from the phase plots must be considered inconclusive.

Compressors 6 and 8 show clear periods of travelling. This travelling is not straight-line in nature, but rather occurs in a 'stair-step' fashion. Compressor 4 exhibits similar stair-step behavior, as well as some travelling in the negative direction (against rotor rotation). Simulations have shown that this behavior is typical of compressors which are operating in distorted flow (Boussios, 1993). Note particularly the magnitude plots for compressors 6 and 8, which exhibit cyclic amplitude behavior, with the period of the cycle being approximately twice per revolution of the waves. This behavior is also typical of distorted flow operation, because the wave amplitude varies as it travels around the annulus due to the non-uniform flow conditions.

Data taken at lower corrected speed (Fig. 5) show a different picture of stall inception. In all cases, pre-stall travelling waves are both large in amplitude (note the pre-stall period jumps in wave amplitude that occur in compressors 4 and 5, which are noticeable, but still much smaller than the jumps that occur at stall inception) and coherent (periods of straight-line travelling of 10 revolutions or more appear in all of the runs). Stall warning times are also longer. As can be seen in the two separate runs of compressor 4, the warning times are not repeatable using this simple straight line phase plot technique.

PRE-STALL POWER SPECTRA

We have delineated and demonstrated the pitfalls of using spatial Fourier coefficient phase for investigating the existence of pre-stall waves. 'Stall warning' times as computed in the previous section do not appear to be attractive for most applications. Much of this may rest with the fact that, although useful in many cases, phase plots can yield misleading and hard-to-interpret results because they are not robust to noise in the system. However, many of the problems encountered in temporal phase plots can be overcome by using the power spectra of the spatial Fourier coefficients, a measure of the wave energy, instead of the wave time history. Power spectra allow behavior over some time window to be computed, and thus show the existence of *stochastic* travelling waves, rather than relying on the appearance of deterministic waves. Specifically, we use the area difference between the positive-frequency and negative-frequency spectra (the shaded area in Fig. 2) as a clear indication of the amount of spectral energy which is travelling relative to that which is stationary - we term this area difference the 'travelling wave energy' (see Appendix A). When this travelling wave energy is in the frequency range important to rotating stall, then sufficient information may be available for a pre-stall warning scheme.

Figures 6 and 7 show the spectra computed from the data in Figs. 4 and 5 in a stationary window approximately 100 rotor periods long ending just before stall inception (recall that the rotor frequency has been filtered from this data). Since these plots contain only the data *prior* to stall inception, no wave energy associated with stall inception or fully developed stall is included. Any travelling is purely due to pre-stall waves. We have again chosen arbitrary scales for the ordinate to facilitate comparison among the plots.

All of the compressors represented in Figs. 6 and 7 show small amplitude travelling wave energy prior to stall or stall/surge inception at both 100% and 70% speed. Thus modeling small-amplitude wave behavior is a potentially useful method for describing pre-stall compressor behavior. A physical interpretation of such a spectrum is that a shaded peak indicates a wave rotating about the compressor at the designated speed. The wavelength of the disturbance is the compressor circumference divided by the spatial harmonic number (k). Some of the compressor data for a single harmonic agrees quite closely with the very simple model of Eq. (3) that is illustrated in Fig. 2. For example, the 7-stage compressor in Fig. 6 has (1) a first spatial harmonic wave (wavelength = compressor circumference) rotating at 0.7 times the shaft speed, and (2) a second harmonic wave (wavelength = 1/2 circumference) rotating at 1.7 times shaft speed. Other compressors show multiple waves at a single spatial harmonic, as is the case for the 5-stage machine in Fig. 6. Overall, it is clear in Figs. 6 and 7 that travelling wave energy is often much more broad-band and complex than would be expected if only a single harmonic mode (eigenvalue) were involved in the stall inception processes as the wave damping approached zero (as Eq. (3) and Fig. 2 assume). Note particularly in Fig. 6 that compressors 4, 5, and 8 exhibit extremely broad-band travelling behavior, and this accounts for the lack of distinct travelling in the phase plots for these compressors in Fig. 4. Even when a single peak is evident in the plots, it is often much wider than one would expect if the damping ratio of a single mode were close to zero (compressor 1 in Fig. 6, and all of the 70% cases).

ROTATING WAVE ENERGY AND COMPRESSOR STABILITY

For some of the compressors discussed here, we have

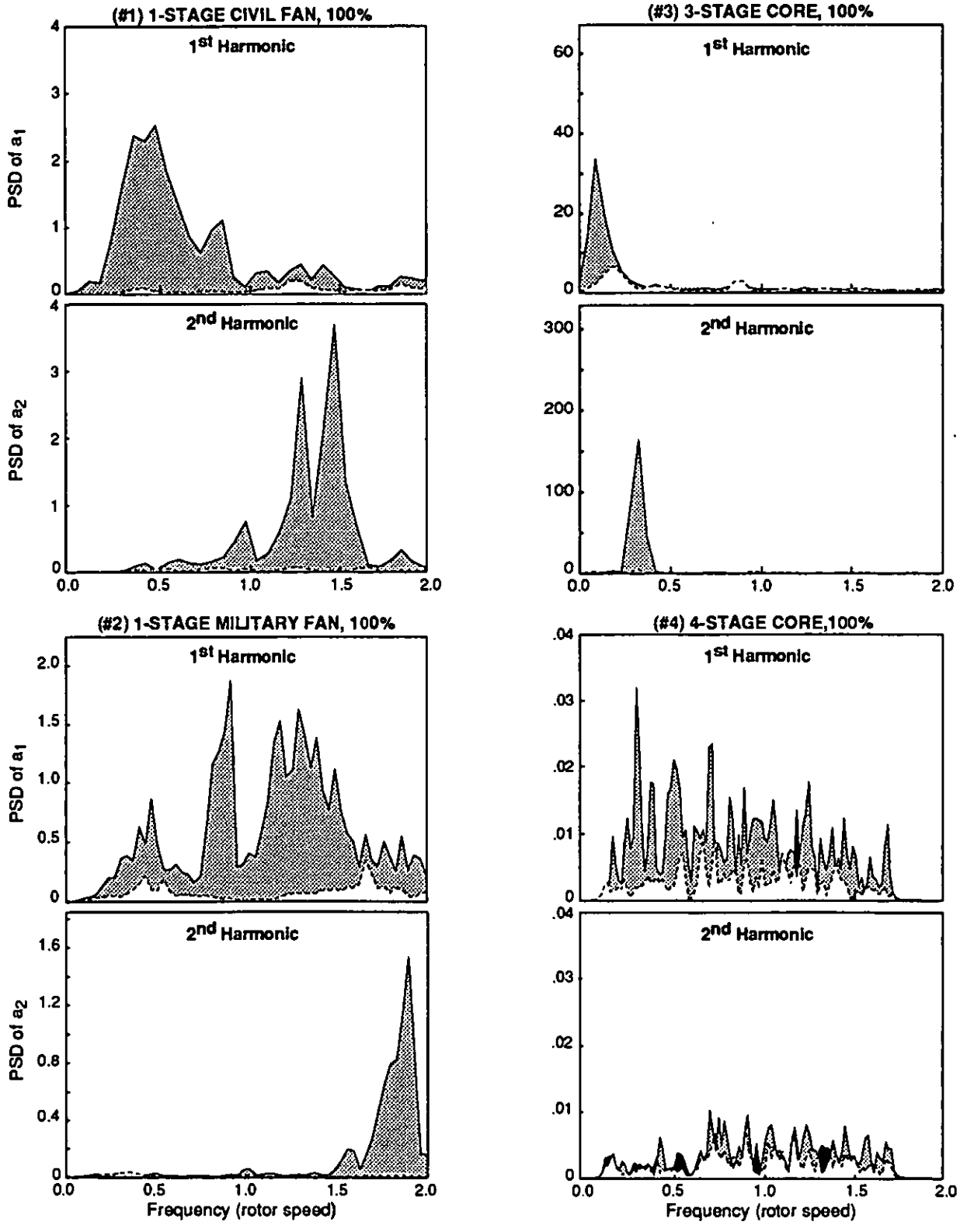

Fig. 6: Pre-stall spectra of first and second Fourier coefficients (PSD of a_1 and a_2), same data as Fig. 4. Solid line is positive frequency spectrum, dashed line is negative frequency spectrum. Gray areas: forward travelling wave energy; black areas: negative travelling wave energy; white areas: stationary wave energy.

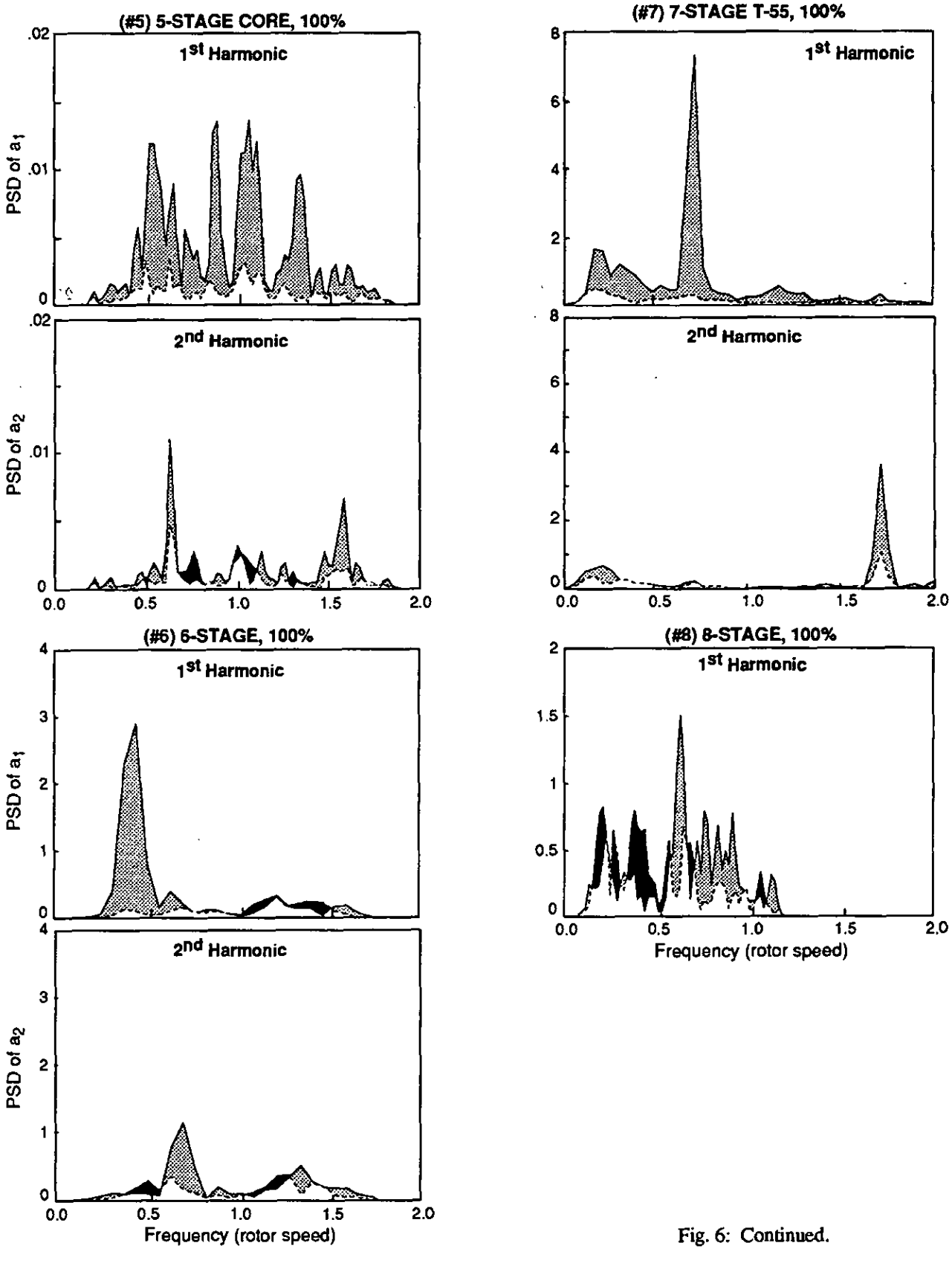

Fig. 6: Continued.

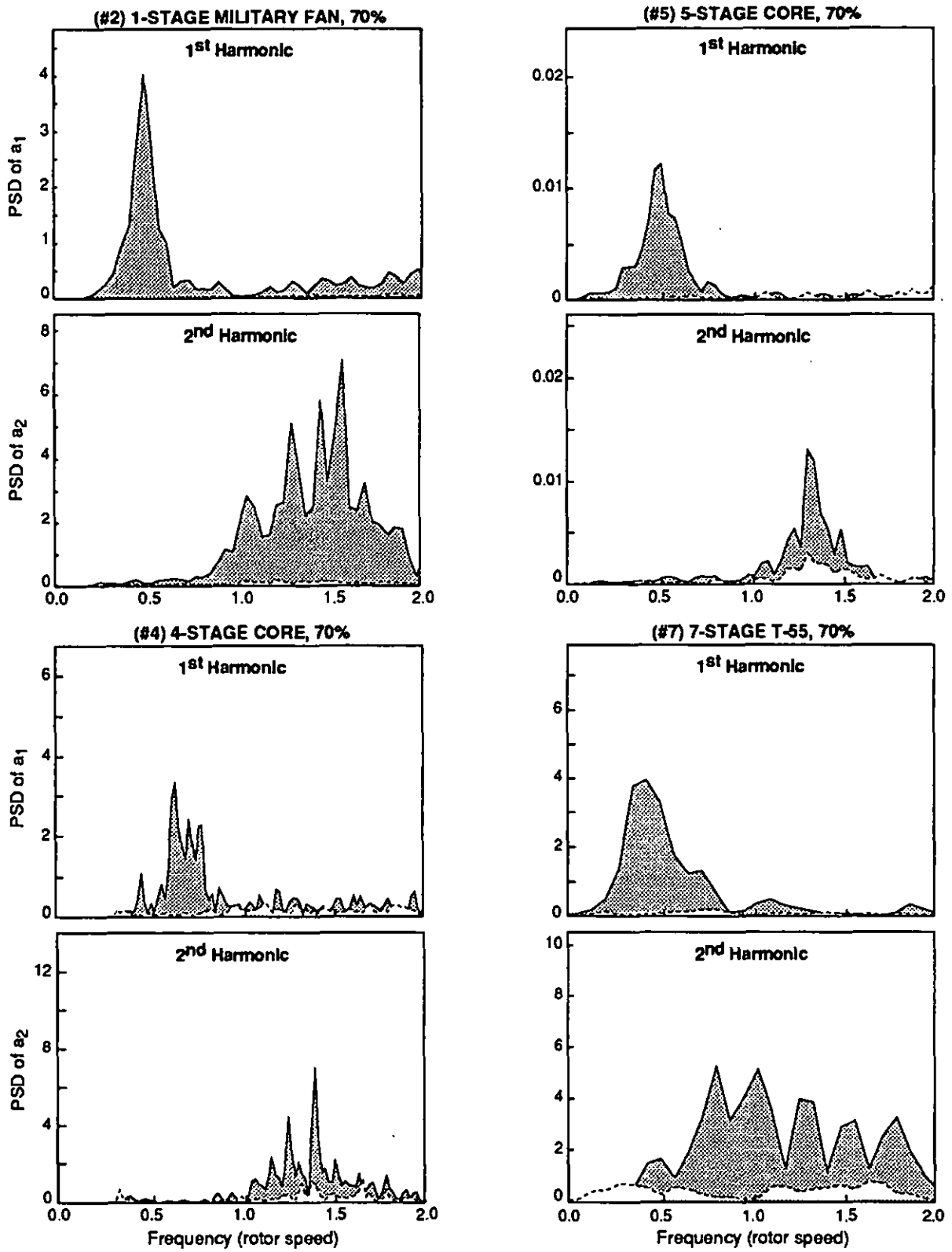

Fig. 7: Pre-stall spectra of first and second Fourier coefficients (PSD of a_1 and a_2), same data as Fig. 5. Solid line is positive frequency spectrum, dashed line is negative frequency spectrum. Gray areas: forward travelling wave energy; black areas: negative travelling wave energy; white areas: stationary wave energy.

data taken continuously during throttle traverses from full open to surge/stall along a constant speedline. A convenient way to examine this information is in the form of a 3-D "waterfall" spectral plot. Here, the power spectrum of a spatial harmonic is calculated over a window of fixed period (50 rotor revolutions in this case) and plotted as in Figs. 6 and 7. The window is then marched forward in time by a period of a few rotor revolutions and the process repeated. The result is a presentation of the variation of the rotating spatial wave spectral distribution over time and therefore (in this case) as a function of throttle or speedline position. Shaft frequency is not filtered out.

Figure 8a illustrates such a speedline traverse from wide open throttle through rotating stall for the 4-stage compressor at 70% corrected speed. The large peak at 0.7 times shaft rotation frequency is readily identifiable as rotating stall in this machine. Little rotating wave energy is evident in this figure prior to stall. However, when the pre-stall period is replotted at an amplitude scale expanded by a factor of 50 (Fig. 8b), rotating waves are readily apparent for the entire time. Rotating wave energy is seen at both 0.7 and 1.0 times shaft frequency, even far away from stall (1000 revs) with the 100% wave being the strongest. As stall is approached, the energy at both frequencies rises sharply and energy appears at 0.5 times shaft frequency as well. (Note also that there may be some nonlinear intermode coupling in that the 0.7 and 1.0 frequencies appear to beat against each other.) Once the stall initiation process starts, it is the 0.7 frequency wave which evolves into rotating stall.

The pre-stall behavior of this 4-stage compressor is a strong function of corrected rotor speed. Figure 9 shows the circumferential travelling wave spectral time histories during throttle traverses at four corrected speeds. At all speeds, waves travelling at both 0.7 and 1.0 times shaft speed are present throughout and rise sharply just before stall initiation. However, the strength of the 1.0 relative to the 0.7 frequency wave is much larger at 100% corrected speed than at lower speeds (200:1 compared to 6:1). Repeated test runs of this compressor confirm that this wave structure is consistent. (In some tests, the 0.7 wave rises just prior to stall by a factor of 5~10 times that shown in Fig. 9.)

How general is this behavior? Data from throttle traverses of four compressors are shown in Fig. 10. The single-stage (#2) and 5-stage (#5) compressors show behavior similar to that of the 4-stage machine. At 70% speed, the single-stage compressor data (Fig. 10a) shows waves rotating at 0.5 and 1.0 of shaft speed. The 0.5 frequency wave grows as the throttle is closed until it develops into rotating stall. At 100% corrected speed, the 1.0 shaft frequency wave completely dominates the spectrum, growing in amplitude as stall is approached. (The stall speed is 0.5 times rotor frequency at both corrected speeds.) The 5-stage compressor (Fig. 10b) differs only in that the 1.0 shaft frequency wave is barely detectable at 70% corrected speed. The 0.7 frequency wave dominates, growing in strength as the throttle is closed to rotating stall. As with the 1-stage and 4-stage compressors, the 1.0 shaft frequency wave dominates the spectrum at 100% corrected speed, growing in amplitude as stall is approached.

The 7-stage, T-55 data (Fig. 10c) looks somewhat different in that 1.0 frequency wave is always much stronger than the lower frequency disturbance (0.5). At 70% corrected speed, the 0.5 frequency wave is only discernible for a few hundred rotor revolutions before stall. At 100%

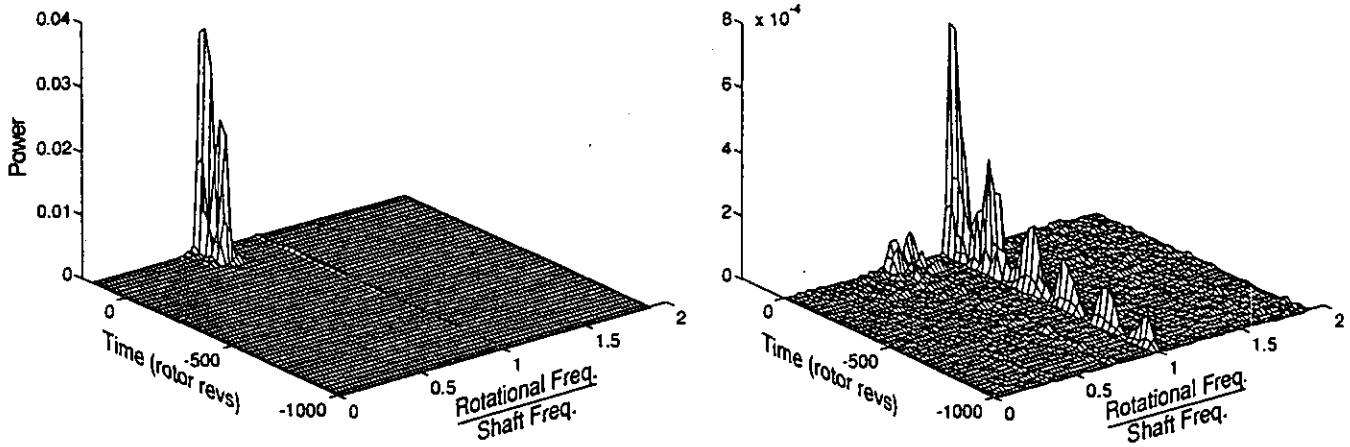

a) 4-Stage, In Stall

b) 4-Stage, Pre-Stall Region

Fig. 8: Time evolution of the PSD of the first spatial Fourier coefficient, a_1, for the 4-stage compressor at 70% corrected speed.

speed, the growth of the 1.0 frequency wave with throttle closure is less pronounced in the other three compressors. Note that a 0.7 frequency wave is still there, but cannot be readily discerned on the scale of Fig. 10. When the shaft frequency is filtered out as in Fig. 6, the lower amplitude wave is apparent. Lower frequency disturbances grow just before stall initiation and also there is a clearly discernible wave travelling at 1.6 times the shaft speed. Reasons for the apparent differences in dynamic behavior between this and the other three compressors may lie in geometry (this is a mixed flow – 7-stage axial, 1-stage centrifugal – compressor, the others are just axials) and/or in sensor placement. (This data is from stage 3 sensors – the furthest back data available – while data from other compressors have shown that part-speed waves are best detected toward the rear of the compressor, especially at 100% speed.)

Viper engine data (Fig. 10d) is similar to that of the T-55. Here, part speed waves appear along with the 1.0 per rev at low corrected speed (81%), but at high speed (98%), the 1.0 rotor frequency wave dominates. As with the T-55, the rise in energy in the 1.0/rev wave is gradual as stall is approached. Day and Freeman (1993) reported that this compressor exhibits short (relative to the compressor circumference) wavelength rotating disturbances prior to stall, which are not readily detected with this type of analysis since the short wave energy is spread over several spatial harmonics.

RELATING THEORY TO EXPERIMENT

How can the measured dynamic behavior exhibited in Figs. 8-10 be explained? Are the features in the data which are common among compressors more important than those which are different? Of what use is this type of data representation? In particular, what is the significance of the disturbances at shaft frequency? (One explanation would dismiss the engine order waves as disturbances resulting from geometric nonuniformities in the rotor. The change in amplitude of this 1/rev wave as the throttle is closed would be a reflection of the aerodynamics changing along a speedline.) We believe that a useful approach is to compare these measurements with a theoretical model of compressor stability.

Hendricks et al. (1993) have developed a compressible version of the two-dimensional, linearized hydrodynamic stability model of Moore and Greitzer (1986). This approach treats the compressor as a series of actuator disks (1 per blade row) separated by inter-blade row volumes, with suitable boundary conditions at the compressor inlet and exit. The 2-D stability of the coupled rows is calculated. Required inputs are the meanline compressor geometry (blade lengths and angles, duct lengths, etc.) and the pres-

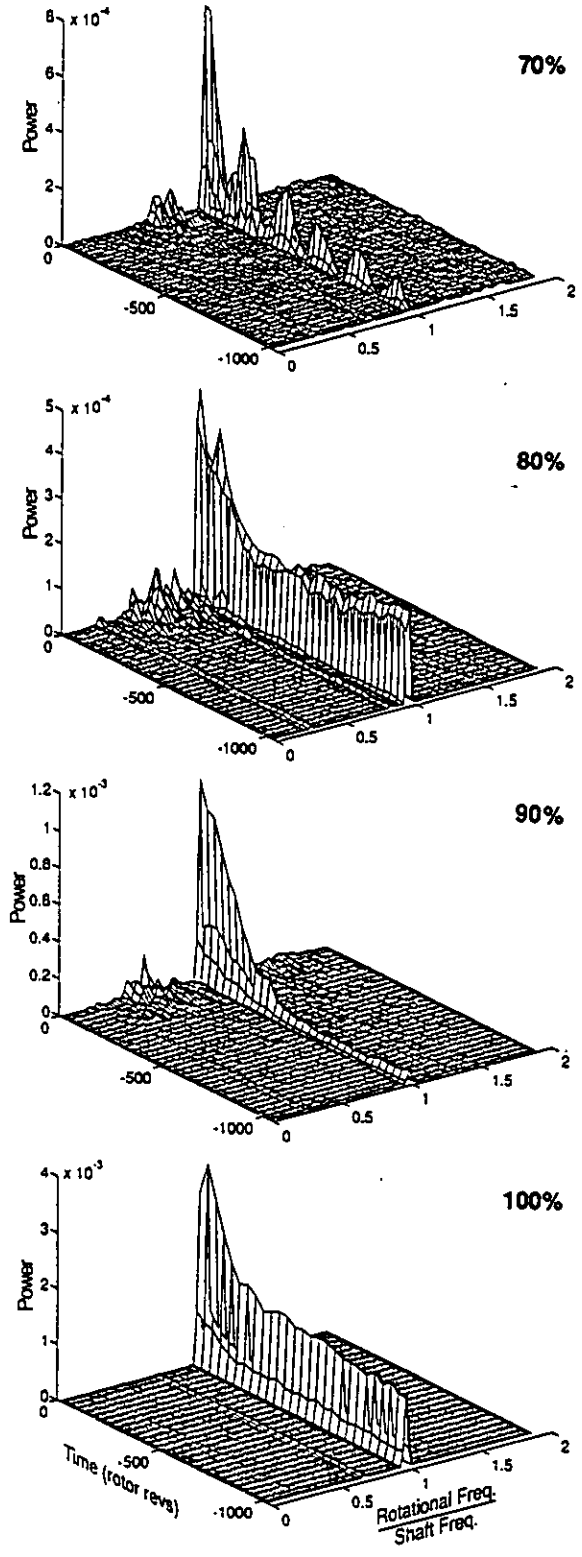

Fig. 9: Influence of corrected speed on the time evolution of first spatial harmonic of 4-stage compressor. Note the change in vertical scales.

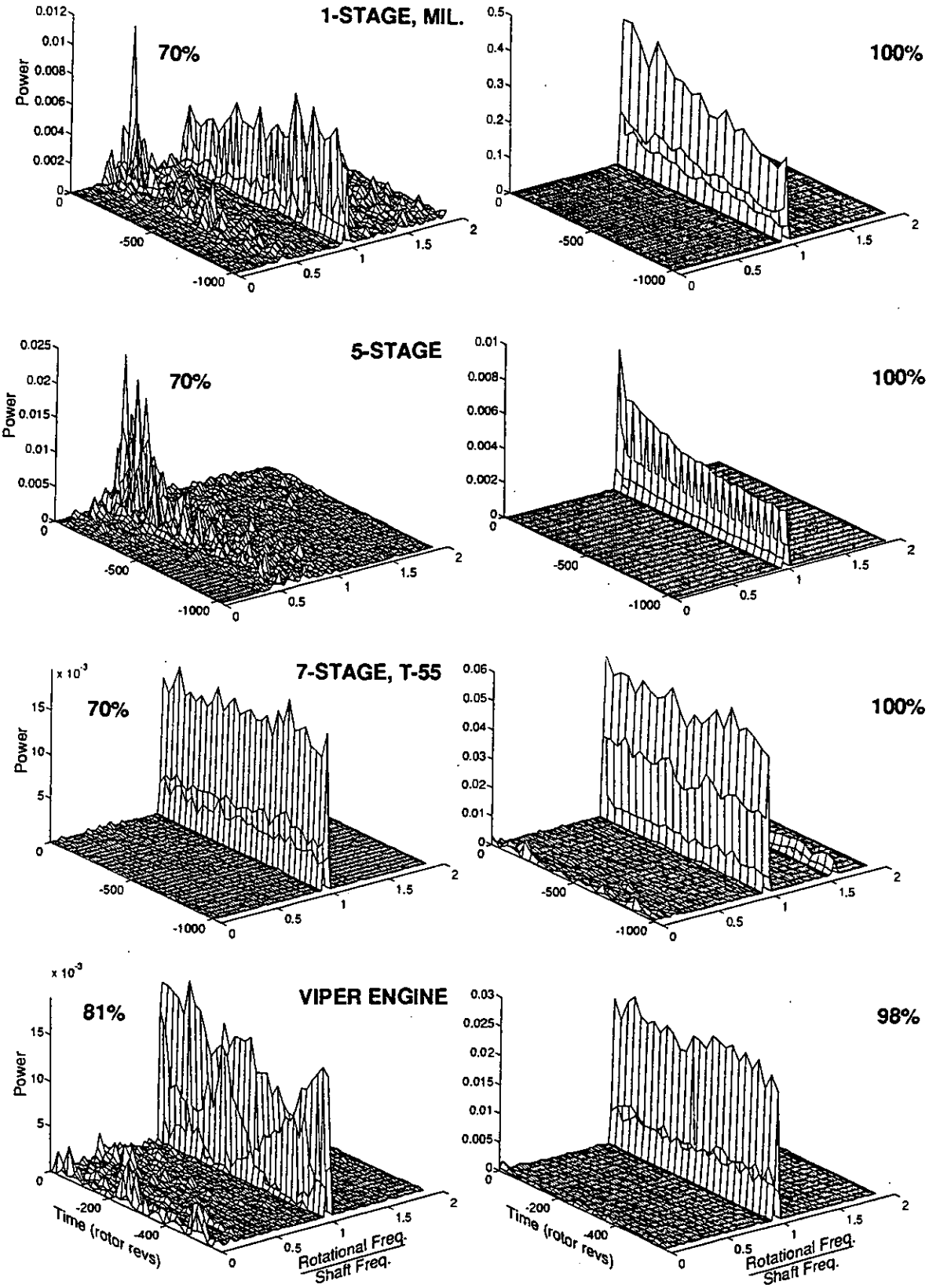

Fig. 10: First spatial harmonic spectra of four compressors at low and high corrected speeds..

sure rise characteristic for each blade row. The results of the calculation include the circumferential *and axial* shape of each spatial harmonic wave, the wave rotational frequency, and the wave growth rate. The calculation is linear so that the dynamics of each spatial harmonic are assumed to evolve independently. Since we are concerned here with the pre-stall region, in which the wave amplitudes are two orders of magnitude below that of rotating stall, the assumption should not pose a problem (Bonnaure, 1991).

We have applied this theory to the geometry of the 4-stage compressor. The individual blade row characteristics have been estimated by a meanline flow calculation (and may thus be subject to some uncertainty). In contrast to the incompressible case, there are an infinite number of natural oscillatory (eigen) modes (as there are by analogy for a duct acoustic calculation) Physical reasoning or intuition must be applied to identify those (hopefully) few modes which control the dynamics of interest. The lowest frequency mode (which we will designate [1,0] by analogy with duct acoustics) has a circumferential wavelength equal to the compressor perimeter and is uniform in structure along the compressor axis. This is the mode familiar from the Moore-Greitzer analysis. It is the only mode that exists in an incompressible machine. (The second incompressible spatial harmonic would be the [2,0] mode, etc.) The addition of compressibility now permits axial structure in the wave form. The next lowest mode is therefore [1,1] with a circumferential wavelength equal to the compressor perimeter and an axial wavelength set by the compressor length (taking into account the inlet and outlet ducts). We will confine ourselves only to these two modes at present since damping tends to increase with mode number and therefore the lower modes are usually the most important.

Figure 11 presents in two ways the results of these calculations of the stability of the first spatial harmonic in the 4-stage compressor. The variation in wave damping ratio (ζ) with compressor mass flow at 70% corrected speed is shown in Fig. 11a. The compressible [1,1] mode is lightly damped even at high mass flows, and its damping ratio decreases as the flow in the compressor is reduced. The incompressible [1,0] mode is highly damped away from stall, but its damping ratio drops more rapidly than that of the [1,1] mode as the compressor is throttled. The result is that the incompressible [1,0] mode goes unstable first at 70% corrected speed. The companion root locus plot of Fig. 11b shows how the wave growth rate and rotation rate vary with compressor mass flow. The incompressible [1,0] mode is predicted to rotate at about 0.5 times shaft frequency, decreasing by about 20% as the compressor is throttled. The compressible [1,1] mode rotates at about 1.4 times shaft frequency and changes little with compressor mass flow. The above picture alters as the compressor speed increases. The compressible [1,1] mode is less stable at 100% corrected speed than it is at lower speeds, and drops more sharply as the compressor mass flow is reduced (Fig. 11c). Thus, the compressible mode goes unstable first at high corrected speed in contrast to the incompressible mode dominating at lower speeds. In addition, the non-dimensional rotational frequency of the compressible [1,1] mode drops as compressor speed is increased so that the natural frequency of this mode is the same as the shaft speed at 100% corrected speed (Fig. 11d).

The experimental data and theoretical calculations form a consistent picture of the dynamics of this machine. The compressor behaves as a multi-mode system excited by forcing with both wide and narrow band components. In this case, a primary forcing is at shaft frequency and is presumably the result of geometric nonuniformities in the flow path. The measured unsteady compressor flow at this frequency reflects both this forcing and the resultant dynamic response of the compressor.

The new result here is that compressible modes can exist in a high speed compressor and dominate the stability at high corrected speeds. Furthermore, different modes appear to be stability-limiting at different speeds. It is also important to note that the compressible mode of interest here behaves differently than the incompressible mode familiar from the Moore-Greitzer analysis and low speed compressor experiments. Specifically, the rotational rate of the compressible mode is fixed while that of the incompressible mode scales with shaft speed (0.5x). The numerical value of the compressible wave speed is approximately coincident with shaft frequency at design speed for this compressor, implying that this mode is very susceptible to forcing due to geometric imperfections in the rotor or eccentricity in the flow path.

We have learned many lessons from the study of this compressor. There are many more modes in a high speed compressor compared to a low speed machine. Which mode dominates the stall inception processes can be a function of compressor speed because of the dependence of the compressor system dynamics – mode frequency, system forcing, and mode damping – on the compressor operating point. In addition, calculations suggest that the upstream and downstream ducting can play a role in the modal dynamics. This implies that the same compressor may exhibit differing stability depending upon the installation, engine versus rig for example, or even different rigs. (This is well known for zero order surge instabilities but less widely recognized for rotating stall and stall initiation.) A major question is the generality of these findings. Are compressible modes the stability limit at high speeds for all, most, or some compressors? Is the coincidence of

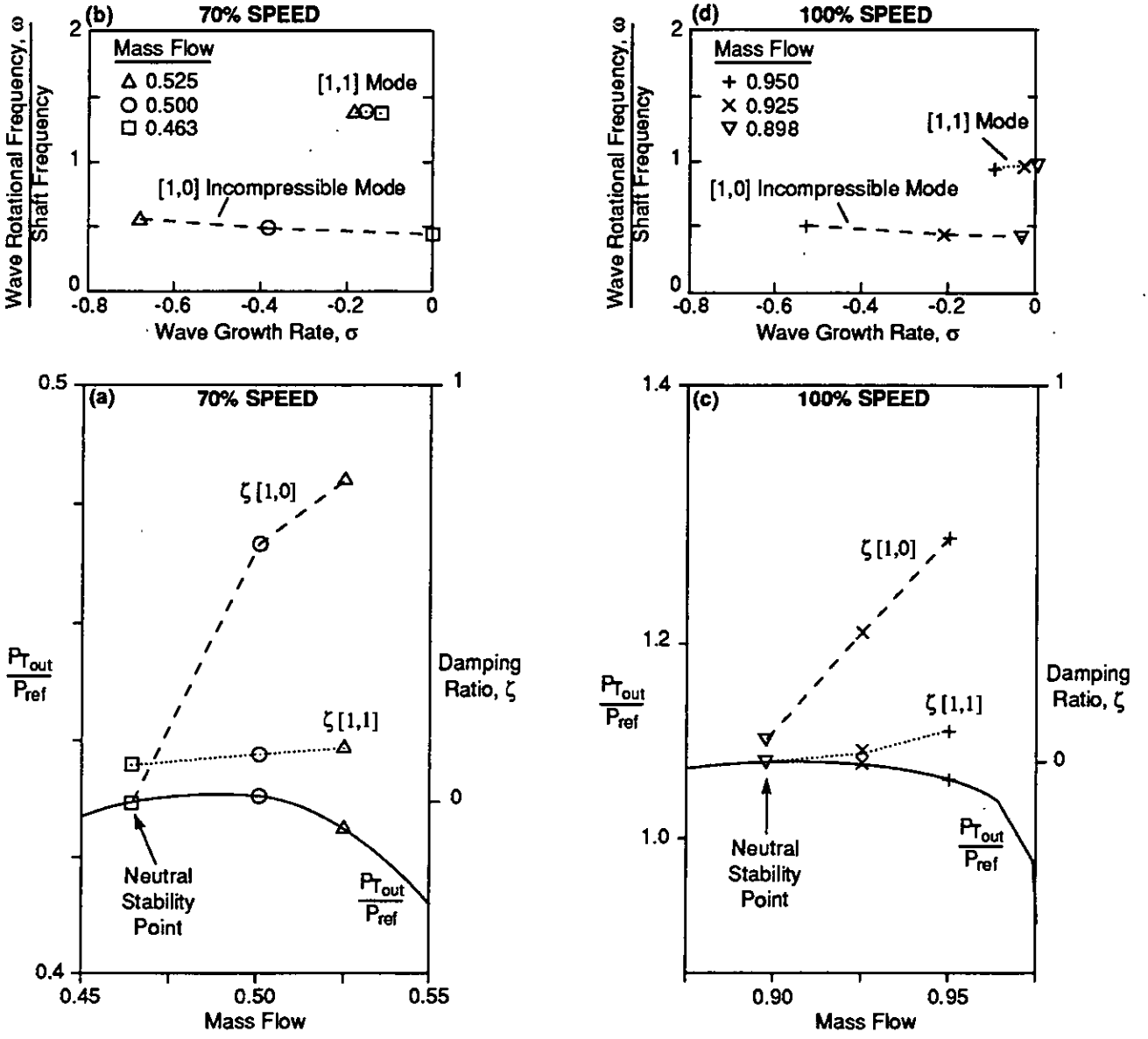

Fig.11: Calculated influence of corrected speed on the first spatial harmonic mode structure of the 4-stage compressor.

mode and shaft frequency at design speed peculiar to the compressors studied or is it more general due to design space limitations? The analytical model predicts that the compressible mode frequencies (ω) vary inversely with compressor length-to-diameter ratio (L/D). The rotational Mach number of the mode ($\omega r/a$) is a constant, independent of rotor speed (U). Thus, as the tangential Mach number of the rotor is reduced toward zero, the normalized mode rotational frequencies ($\omega r/U$) move toward infinity, so that the compressible modes do not participate in the dynamics of low speed (i.e. incompressible) machines. The 4-stage compressor modelled here has an L/D of about 0.5 and a tangential Mach number of 1. Since these values are typical of many high speed, multi-stage compressors, the approximate coincidence of shaft and compressible mode frequencies observed here may be widespread among such machines. The 1-stage and 5-stage compressors in Fig. 10 show the same behavior as the 4-stage machine. (We have analyzed the 5-stage compressor with the stability model which predicts dynamics similar to those in the 4-stage machine.)

The Viper compressor behavior shown in Fig. 10 is

also similar in that it exhibits a pre-stall response at 0.4 and 1.0 of shaft frequency. At high speed, no energy is evident below shaft frequency although response can be clearly seen at higher frequencies. (Viper spectra show narrow band response at discrete frequencies up to 10 times the shaft speed. Also, the second spatial harmonic spectrum is very rich with waves growing as stall inception is approached.) Since we do not have the geometry of this compressor, we have not been able to identify particular modes. At low corrected speed, the T-55 shows weak response at 0.4 times shaft frequency prior to stall initiation. At high speed, no energy is evident below shaft frequency, but response appears at 1.6 times the shaft speed. We are in the process of modelling this compressor to explore this behavior further. Also, the T-55 data shown in Fig. 10 was taken with relatively little throttle motion, near the stall point, and thus does not represent as wide a sweep along the speedline as is the case for the 1-, 4-, and 5-stage compressors. More work needs to be done here.

Overall, these multi-stage, high speed, axial compressors are rich in modes (eigenvalues), most of which do not exist in low speed compressors. Detailed analysis is needed on each geometry to elucidate the physical significance of each mode and its importance to instability inception at any particular speed. It is clear, however, that modal response is exhibited by all of the machines studied.

USING 'WAVE ENERGY' AS A STALL WARNING

We have seen that prior to stall, significant travelling wave energy exists in all of the compressors studied and that this energy changes with operating point. The question is: can this travelling energy be used as a stall warning indicator? One straightforward approach is simply to calculate the travelling wave energy as a function of time and then threshold this level at some appropriate value. This was done for a fixed-length time window in which the spectrum of the desired spatial Fourier coefficient was estimated (only data prior to the time sample was used so that the filter was causal). The integrated travelling wave energy for frequencies between 25% and 125% of the rotor frequency was then calculated from the spectrum (the positive area minus the negative area in Fig. 6) and assigned to that point. The window was then marched forward in time by one point and the process repeated. Since the raw compressor data is noisy, the length of the spectral window influences the variance of the wave energy estimate. The longer the window, the less the variance. Too long a window, however, will smooth out the transients of interest. Although we have not made a quantitative analysis of this tradeoff, we have found a 50 rotor rev window to be a workable compromise between reducing the noise and losing the detail of the pre-stall transient.

The time history of the travelling wave energy in the first spatial harmonic was so calculated for data taken during slow throttle traverses from full open to stall for the 4-stage compressor. Figure 12 shows such a time history of the integrated wave energy at four corrected speeds. In all cases, the wave energy rises steeply at 100-200 rotor revolutions prior to stall. At 70% and 75% corrected speeds, the mean d.c. level is approximately constant during the throttle closure until the abrupt pre-stall rise. At 80% speed, the d.c. level drops for 1000 revs prior to stall (this is the only data set we have which behaves in this manner). At 100% speed, the d.c. level rises slowly as the throttle is closed until the more abrupt pre-stall rise. For some cases, we have multiple data sets at similar conditions. These can show a factor of two or so in the length of the pre-stall period of increased wave energy. (The shortest periods are illustrated here.)

To use this integrated wave energy concept as a stall warning indicator, we must set a threshold level in some manner. This requires some care as the wave energy time trace is noisy. Figure 13 shows the data from Fig. 12 replotted on an expanded scale. Here the very simple approach of adopting a level just higher than the highest peak observed before 200 revs prior to stall is used. This yields warning times on the order of 100 to 200 revolutions prior to stall initiation, even at 100% speed. For conditions at which we have multiple test runs, these results represent the shortest warning period. We believe that these are con-

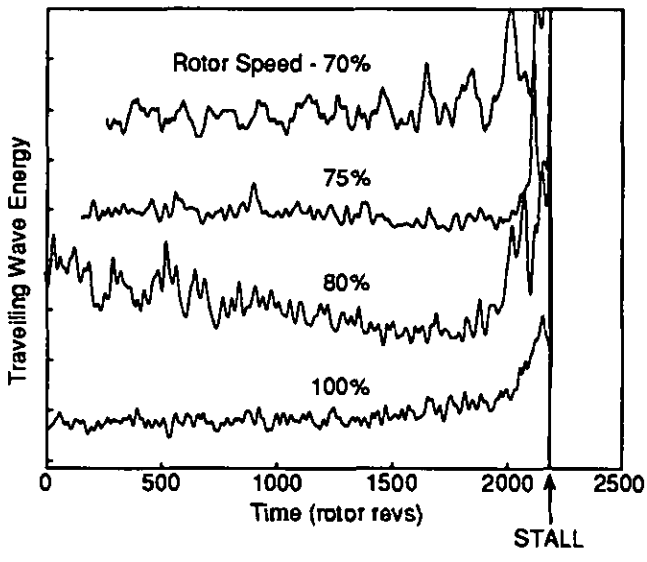

Fig.12: First spatial harmonic travelling wave energy during slow throttle traverse into stall for a 4-stage compressor.

servative values and that more sophisticated signal processing (removing the high frequency spikes, incorporating the low frequency d.c. level changes, for example) should yield considerably longer warning times for data such as that analyzed here.

Since the throttle closure rate was constant during any single test run and the pressure rise and mass flow were measured, the operating point along the speedline at the time corresponding to the stall warning period could be determined. At 100% speed, the warning period was equivalent to about a 0.2% change in mass flow. Data was analyzed for 100% speed tests in which the throttle rate varied by a factor of thirty (the rate was constant during any single test). The data from all tests behaved similarly in that the d.c. level of the integrated wave energy rose slowly until a more abrupt rise immediately preceding stall initiation. The level correlated with operating point on the speedline so that amplitude of the wave energy was found to be high for proportionately longer at low throttle rates than at higher ones. For this compressor, at least, the level of wave energy is clearly a function of the position along the speedline.

Overall, these results are very encouraging. They show that travelling wave energy can be used to identify pre-stall waves in high speed compressors, even at the highest rotational speeds and throttle rates – conditions at which examination of time traces and Fourier coefficient histories have proven unreliable. Furthermore, increased wave energy is discernible for a significant time (at least 100-200 rotor revolutions) before stall in all cases. More

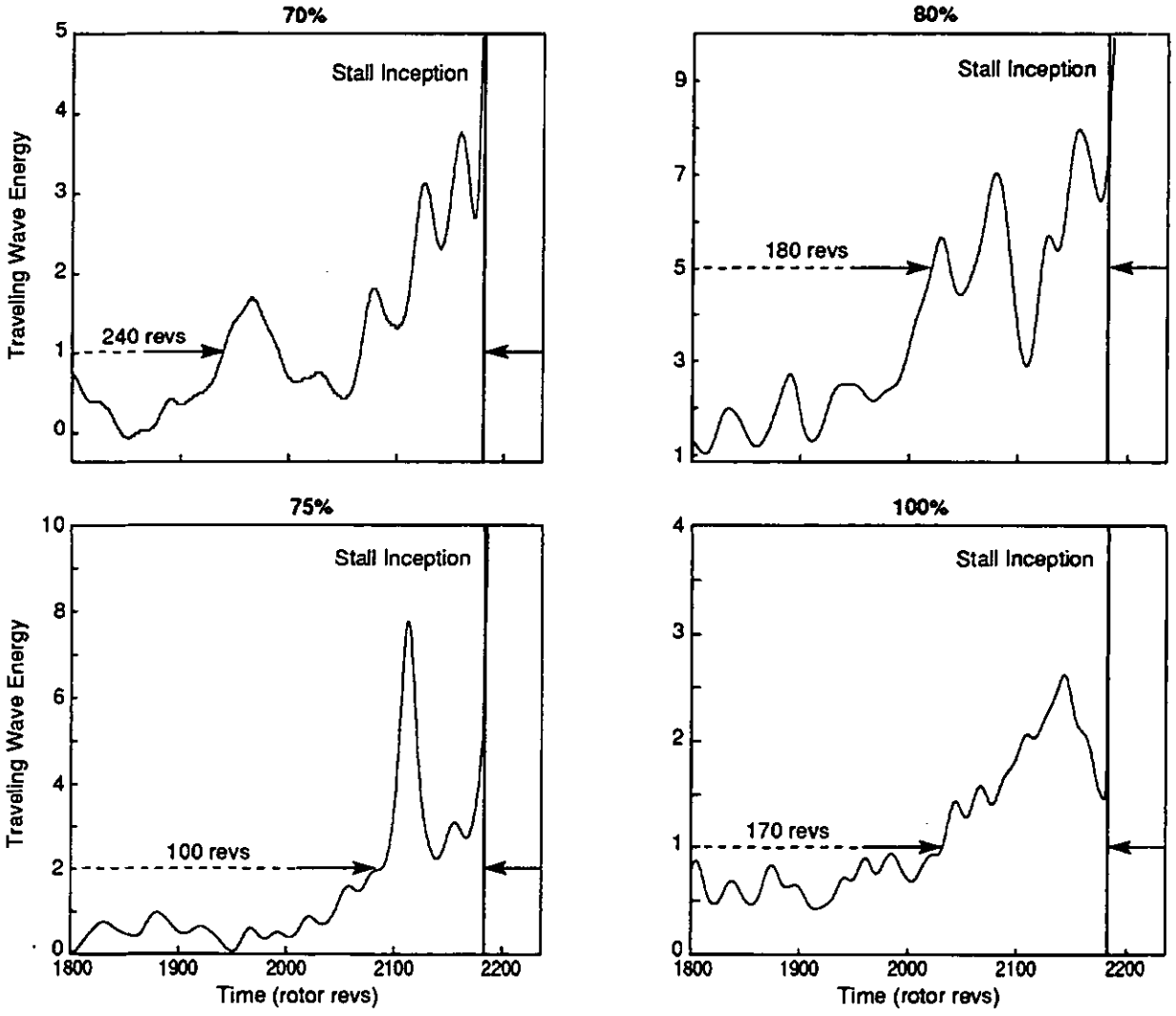

Fig.13: Data of Fig. 12 replotted on an expanded scale illustrating stall warning times prior to stall inception.

work needs to be done in the signal processing of these somewhat noisy signals before they could be considered a reliable stall warning. The signal-to-noise ratio can be improved through judicious selection of the spatial harmonics and modes included in the wave energy calculation for any given compressor. Also, more sophisticated signal processing could be applied.

DISCUSSION

The coherent picture which has emerged from these experimental and analytical studies is that the compressors examined behave like multi-mode, oscillatory, dynamic systems in the small amplitude pre-stall region. We would now like to discuss the implications and limitations of this physical model on compressor design and stall warning.

The specific mathematics used here are derived from the linearized approach of Moore and Greitzer so that they only apply to the small signal regime preceding stall inception. The stall inception process, as the waves grow to large amplitude, fully-developed rotating stall, is not described by this model. (It would also be inappropriate for describing the dynamics of the part-span rotating stall found in some compressors prior to surge or large amplitude stall.) In particular, the assumption that the dynamics of each spatial harmonic and each mode evolve independently is no longer true as the wave amplitude grows. This is readily seen in the data in which pre-stall energy at shaft speed evolves into 0.5 times shaft speed rotating stall through nonlinear mode coupling. A second assumption, that the flow can be described by a two-dimensional model, can also be limiting, especially in low hub-to-tip ratio compressors. The addition of a third spatial dimension enables additional resonant modes, and we have seen some evidence of such modes in the data from fans. Although it appears that a two-dimensional mode first goes unstable in the machines examined here, it is certainly conceivable that a three-dimensional mode might be the most critical in other compressors.

Historically, attention has been focussed on fully developed rotating stall and surge or, more recently, on the stall inception processes. But in a very real sense, it is the pre-stall region which is the most interesting since the design intent for a compressor is to avoid instability – at whatever penalty in performance, weight, or cost that must be incurred. In many ways, the pre-stall fluid dynamic stability of the compressor can be viewed in a fashion analogous to its structural dynamic stability. In both cases, the compressor is a system rich in closely spaced, orthogonal modes operating in the presence of strong forcing. The point is not that the particular mode structure described in Fig. 11 is universal (which it surely is not), but that (1) many modes can exist simultaneously, and (2) which mode limits stability is a function of operating point and performance details.

In our 2-D representation, the mode structure and damping are set by the compressor mean line geometry and the blade row speedlines. As can be seen in Fig. 11, two or more modes may have very low damping simultaneously. The stability of the compressor may thus be set by the influence of the external forcing on the modes, which is beyond the scope of linear theory. In addition, precise prediction of mode damping is difficult since blade row speedline slopes cannot now be accurately estimated near the stall line. However, the influence of geometry changes on the relative compressor stability is often useful in design and this can now be assessed. For example, the modelling indicates that the modal damping is sensitive to axial loading distribution. Also, reduction of losses, blockages, and deviation all help to increase the speedline slope and therefore increase stability.

The aerodynamic forcing of the compressor modal dynamics is an important consideration in establishing the overall system stability. Dynamic systems as described here can be driven unstable when in a normally stable operating regime by external forcing of sufficient amplitude. With the exception of inlet distortion, the perturbation structure in compressors has not been studied in the context of compressor stability. Thus, it is currently difficult to characterize a particular machine as being weakly or strongly forced for this purpose. We do know, however, that compressors are very noisy and perturbations of several percent of the mean flow are not uncommon, especially at harmonics of shaft frequency. Manufacturing uniformity and uniformity of tip clearance may influence this forcing and therefore affect compressor stability.

The system dynamic response to forcing can be studied analytically. Even at damping ratios which are greater than zero, wave magnitudes can become large enough that they elicit a *nonlinear* response of the system. In this case the linear stability of the system is intact, but the nonlinear stability, or resistance to perturbations of finite magnitude, is very delicate. Mansoux et al. (1993) have studied this possibility by developing a Lyapunov stability analysis of the Moore-Greitzer model. When the so-called 'domain of attraction' of the operating point becomes very small, perturbations which might be considered 'linear' in magnitude can actually be unstable due to nonlinear effects. Thus it is not the damping ratio alone, but the increased perturbation level associated with low damping ratios *combined* with degradation of the nonlinear resistance to such perturbations, which determines the rotating stall inception point.

Much of the analysis to date has concentrated on the modal structure of the first spatial harmonic. For many

compressors, rotating stall consists of two or more stall cells so that high order spatial harmonics can also be important. Second spatial harmonic waves are readily apparent in the data, in both the spectra in Fig. 6 (compressors 1, 3, 5, 6, and 7 for example) and even in the phase time history plots in Figs. 4. and 5 (compressors 3, 6, and 7). The higher harmonic waves travel at the same rotational speed as the first harmonic and are thus susceptible to the same forcing. Another concern is the short length scale disturbances during stall inception, reported in the Viper engine by Day and Freeman, and by Day in low speed compressors, which may also play a role. These may be either a three-dimensional response of the system or represent system forcing which triggers stall. These disturbances seem more properly a part of stall inception rather than pre-stall as they appear in the last few rotor revolutions before stall and have amplitudes relatively large compared to the pre-stall waves. As mentioned earlier, the data analysis techniques applied here are not well suited to the detection of short length disturbances since their energy would be spread across many spatial harmonics. Issues such as these deserve further study and time constraints prevented their inclusion herein.

CONCLUSIONS AND SUMMARY

In this paper, we have examined pre-stall data from nine, high speed compressors, representing fans, core, and engine compressors from four different manufacturers, and encompassing many variations in design philosophy, number of stages, hub-to-tip ratio, and loading. While these differences do effect many of the details of the data, significant similarity exists, and these similarities are the focus of this paper. In particular, our focus has been on the steady, pre-stall inception dynamics of these compressors.

First of all, we have shown that stall precedes surge in all of the compressors tested. This is a conclusion that many researchers have reached based on their own experience, and it is useful to demonstrate that this observation is consistent among many different machines.

We have reviewed several techniques for the detection of small amplitude rotating waves and explained their limitations. A new technique is introduced based on spectral analysis of the spatial Fourier harmonics of measured data. Using this approach, we have shown that:

1) Low amplitude travelling waves are found in all of the compressors prior to stall.
2) The travelling wave structure is different at low and high corrected speeds. Specifically, a wave rotating at 1/2 of shaft frequency grows strongly at low speeds, while a shaft frequency disturbance dominates at 100% speed.
3) At constant speed, the wave structure is a function of the position on the compressor speedline.

A newly developed, 2-D, linearized, compressible, hydrodynamic stability model was used to analyze the geometry of two of the compressors. The analysis results are consistent with the experimental data. Several new findings have emerged, specifically:

1) Additional oscillatory modes exist in high speed compressors compared to the same geometry with incompressible flow.
2) The dependence of mode damping and frequency on operating point is different for different modes.
3) At low corrected speeds, the incompressible mode predicted by the Moore-Greitzer analysis and observed in low speed compressors sets the high speed compressor stability limit.
4) At high corrected speeds, a hitherto unrecognized compressible mode is stability limiting.
5) The compressible mode differs from the incompressible mode in that its frequency is fixed (i.e. doesn't scale with shaft speed) and is approximately coincident with shaft frequency at 100% speed for many compressors.
6) The above implies that the stability of this mode and therefore that of the compressor can be strongly affected by external forcing due to sources such as geometric non-uniformities in the compressor.

Based on the ideas developed through this analysis and data reduction, we have introduced the concept of "integrated travelling wave energy" as a measure of compressor stability. The wave energy is shown to be a function of the position of the operating point on the speedline. Applying this wave energy technique to high speed compressor data consistently gives at least 100-200 rotor revs warning prior to the inception of rotating stall for the data sets tested. When suitably developed, this approach may yield a usable stall warning scheme.

Finally, the data and analysis give a consistent picture of pre-stall initiation compressor stability dynamics behaving as a multi-mode dynamic system. We believe that this representation is of use for compressor design, data analysis, stall warning, and compressor control. Much work remains to be done in more thoroughly testing these concepts and understanding their ramifications.

ACKNOWLEDGEMENTS

This paper could not have been completed without the active assistance of many people and organizations in contributing data and time. We thank S. Baghdadi, J.E. Garberoglio, and D. Hobbs of Pratt & Whitney; W. Copenhaver, D.A. Hoying and D. Rabe of the Wright Laboratory USAF; A. Sehra and S. Etter of Textron

Lycoming; C. Freeman and A. Wilson of Rolls-Royce plc; and K. Owen of the US Army. D. Park thoughtfully prepared the manuscript and figures. This work was supported by the US Air Force Office of Scientific Research, Major D. Fant, program monitor; Pratt & Whitney; and NASA Lewis Research Center.

REFERENCES

Boussios, C.I., 1993, "Rotating Stall Inception: Nonlinear Simulation, and Detection with Inlet Distortion," M.S. Thesis, MIT Dept. of Mechanical Engineering, February.

Bonnaure, L.P., 1991, "Modelling High Speed Multistage Compressor Stability," M.S. Thesis, MIT Dept. of Aeronautics and Astronautics, September.

Boyer, K.M., King, P.I., Copenhaver, W.W., 1993, "Stall Inception in Single Stage, High-Speed Compressors with Straight and Swept Leading Edges," AIAA 93-1870, presented at the AIAA/SAE/ASME/ASEE 29th Joint Propulsion Conference and Exhibit, Monterey, CA, June 29-30.

Day, I.J., 1993a, "Stall Inception in Axial Flow Compressors," *J. of Turbomachinery*, Vol. 115, No. 1, January.

Day, I.J., 1993b, "Active Suppression of Rotating Stall and Surge in Axial Compressors," *J. of Turbomachinery*, Vol. 115, No. 1, January.

Day, I.J., Freeman, C., 1993c, "The Unstable Behaviour of Low and High Speed Compressors," presented at the International Gas Turbine and Aeroengine Congress and Exposition, Cincinnati, OH, May 24-27.

Etchevers, O., 1992, "Evaluation of Rotating Stall Warning Schemes for Axial Compressors," M.S. Thesis, MIT Dept. of Aeronautics and Astronautics, August.

Freeman, C. Wilson, A.G., 1993, "Stall Inception and Post Stall Transients in an Aero Engine Axial Flow Compressor," presented at I. Mech E.

Gallops, G.W., Roadinger, T.J., French, J.V., 1993, "Stall Testing and Analysis of Two Mixed Flow Turbofans," ASME paper 93-GT-62, presented at International Gas Turbine and Aeroengine Congress and Exposition, Cincinnati, OH, May.

Garnier, V.H., Epstein, A.H., Greitzer, E.M., 1991, "Rotating Waves as a Stall Inception Indication in Axial Compressors," *J. of Turbomachinery*, Vol. 113, April.

Greitzer, E.M., Fulkerson, D.A., Mazzawy, R.S., 1978, "Flow Field Coupling Between Compression System Components in Asymmetric Flow," *ASME J. of Engineering for Power*, Vol. 100, pp. 66-72.

Hendricks, G.J., et al., 1993, "Analysis of Rotating Stall Onset In High-Speed Axial Flow Compressors," AIAA paper 93-2233, presented at the 29th Joint Propulsion Conference, Monterey, CA, June.

Hoying, D.A., 1993, "Stall Inception in a Multistage High Speed Axial Compressor," AIAA paper 93-2386, presented at the 29th Joint Propulsion Conference, Monterey, CA, June.

Mansoux, C., Gysling, D.L., Paduano J.D., 1994, "Distributed Nonlinear Modeling and Stability Analysis of Axial Compressor Stall and Surge," to appear, *Proc. of 1994 American Control Conference*, Baltimore, June.

McDougall, N.M., Cumpsty, N.A., Hynes, T.P., 1990, "Stall Inception in Axial Compressors," *ASME J. of Turbomachinery*, Vol. 112, pp. 116-125.

Moore, F.K. Greitzer, E.M., 1986, "A Theory of Post-Stall Transients in Axial Compression Systems, Part I - Development of Equations, and Part II - Application," *ASME J. of Engineering for Gas Turbines and Power*, Vol. 108, pp. 68-97.

Owen, A.K., 1993, "Analysis of Rig Test Data for an Axial/Centrfifugal Compressor in the 12 Kg/Sec Class," presented at AGARD 82nd PEP, Montreal, Canada, October.

Paduano, J.D., 1992, "Active Control of Rotating Stall in Axial Compressors," Ph. D. Thesis, MIT Dept. of Aeronautics and Astronautics, February.

Widrow, B., et al., 1975, "Adaptive Noise Cancelling: Principles and Applications," Proc. IEEE, Vol. 63, December, pp. 1692-1716.

APPENDIX A
POWER SPECTRA OF SPATIAL FOURIER COEFFICIENTS

Spectral analysis of the spatial Fourier coefficients offers a way to discern the nature of the stochastic signals which often occur in axial compressor data. The procedure is to plot the power spectral density (PSD) of each spatial Fourier coefficient during a period prior to stall. The stall event itself is *not* included in the analysis, so the spectra show resonant behavior which exists in the small amplitude behavior of the system rather than the nonlinear limit cycle behavior. Analyzing the spatial Fourier coefficients in this way helps to determine whether waves in the compressor tend to rotate in the way predicted by the linearized theory of compressor dynamics.

Because the spatial Fourier coefficients are *complex* functions of time, the PSDs are not symmetric with respect to zero frequency, as is usually the case. This is true because, for a complex signal., the sign of the frequency has a very specific meaning. In the context of rotating stall, the sign of the frequency indicates the *direction of rotation of the wave*. To see this, consider a k^{th}-mode spa-

tial Fourier coefficient whose spectrum is a delta function at some frequency $-\omega_d$ *alone*, that is, there is no peak at $+\omega_d$. The time domain signal corresponding to this spectrum is

$$a_k(t) = e^{-j\omega_d t}.$$

The signal is complex because the spectrum we started with was not symmetric about ω=0. Converting this spatial Fourier coefficient back into the spatial domain gives the spatial wave which produced the signal:

$$\delta P_x(\theta,t) = \mathrm{Re}\left\{a_k(t)\cdot e^{ik\theta}\right\} = \cos(k\theta - \omega_d t)$$

which corresponds to a rotating wave, *whose direction of rotating depends on the sign of* ω_d. A power spectrum which is symmetrical, on the other hand, indicates a standing wave with oscillating amplitude. For instance, if we take a spectrum which is a delta function at *both* $+\omega_d$ *and* $-\omega_d$ then the corresponding time signal is

$$a_k(t) = e^{j\omega_d t} + e^{-j\omega_d t},$$

which in turn corresponds to the following wave in the space domain:

$$\delta P_x(\theta,t) = \mathrm{Re}\left\{2\cdot\cos(\omega_d t)\cdot e^{ik\theta}\right\} = 2\cdot\cos(\omega_d t)\cos(k\theta)$$

Here we see that ω_d is the rate at which the standing wave *magnitude* changes with time, rather than the rotating rate of the wave.

With this explanation we see that when we plot a spatial Fourier coefficient spectrum, we must plot both the negative and the positive frequencies, preferably flipping the negative frequency plot to overlay with the positive frequency plot. Then, only the peaks which do not exist at both negative and positive frequencies indicate waves which rotate. A given spectral frequency, then, consists of standing wave energy plus some traveling wave energy: the former is measured by the spectral energy that appears in both the positive and the negative spectra, while the latter appears in one but not the other - that is, it is the difference between the two spectra at that frequency. This difference can either be positive or negative, and the sign determines the direction of the traveling wave energy, as discussed above. Figure A.1 gives an example of dividing the spectrum into its constitutive elements. Note that there is a change in sign between the direction of the wave traveling and the frequency of the spectral line - this is due to the fact that $cos(k\theta - \omega_d t)$ represents a wave traveling in

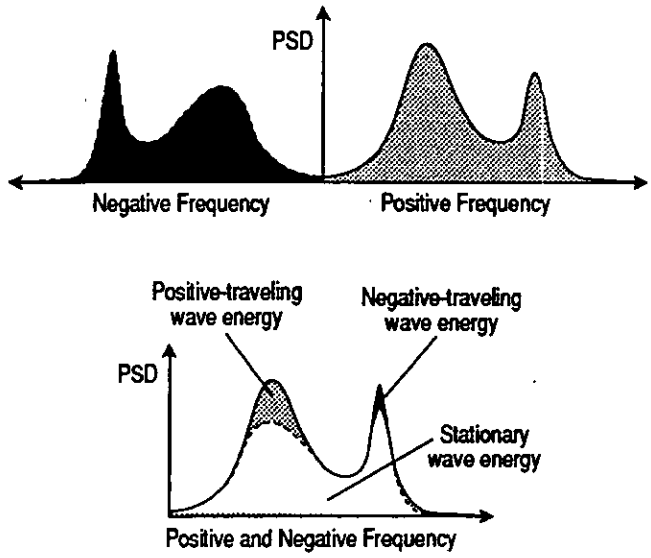

Fig. A.1: An example non-axisymmetric spectrum and its division into positive, negative, and stationary wave energy parts. Note that a peak in the spectrum may indicate resonance which is primarily stationary. In this case, the frequency indicates the rate at which the spatially stationary wave oscillates in magnitude, rather than the wave rotation rate.

the positive direction at a rate ω_d. To avoid unnecessary confusion due to this sign change, we use a slightly different definition of the discrete Fourier transform in our computation of spatial Fourier coefficients, so that both direction of traveling of the phase in a phase plot and the position of the peak in a spectrum correspond to the intuitively appealing convention that positive traveling waves travel with rotor rotation, and negatively traveling waves travel against rotor rotation. Consistency in definition and application of the Fourier transforms is, of course, the key to interpretation of the results in a physically accurate manner.